the initial spectrum of region A, dominated by ice grains in the sub–100 μm size range. The final spectrum (L_s 127.6°) is characterized by a lower albedo and a saturated 2-μm absorption feature, which corresponds to a much larger ice grain size. The best model fit is obtained when ice grains with a size of 700 to 800 μm constitute 70% of the volume. Ice metamorphism cannot explain such a size change in only 1 month (*7*). The most likely interpretation of this spectral evolution is therefore that fine-grained frost constituting the last remnants of the seasonal cap sublimates away, in agreement with models (*15*, *16*). This process exposes permanent ice, which is dominated by large grains (700 to 800 μm). This is similar to what is observed on terrestrial ice caps, such as Greenland, with a correlation between a decrease in albedo and the disappearance of seasonal frost (*17*). Dust contamination at the end of the period is 6% in terms of volume fraction, which is an upper limit because intimate mixture is assumed.

Region C lies within Korolev, one of the southernmost ice-filled craters, at a latitude of 73°N. From L_s 93.6° to L_s 107.4° (Fig. 4C), the spectra are characterized by a flat-bottomed absorption feature at 2 μm; hence, most of the volume (60 to 70%) is occupied by ice grains with sizes in the 700-μm to 1-mm range, similar to the final spectrum of region B. At L_s 93.6°, the observed spectrum has an albedo at 1.085 μm of 46% and an albedo at 2 μm of 6%; hence, the best model fit indicates an initial dust contamination (9% assuming intimate mixture) that is slightly larger than that in region B at the end of its evolution (6%). At L_s 107.4°, the albedo at 1.085 μm has increased to 52%, after which spectral evolution slows down. The albedo at 2 μm of the final spectrum is only 2.5%. Therefore, the upper limit of intimate dust contamination is low (<5%).

If part of the dust is embedded in the ice matrix (intramixture), spectral modeling of the observations leads to a negligible volume fraction of dust ($\ll$1% in all cases), in agreement with (*9*), and the estimated grain size remains the same as with the intimate mixture. If one also takes into account a possible contribution of aerosols, the conclusion is that the residual large-grained ice that is exposed since early summer in outlying regions and 1 month later on most of the ice cap itself is likely to be very clean. Either there is very little dust deposition during the global dust storm season (contrary to what is observed at lower latitudes) or there is an effective clean-up process during sublimation of the surface layers. The decrease in dust contribution that is observed between L_s 93° and L_s 107° in outlying regions (Fig. 4C) supports a surface clean-up process, even if a decrease in the optical thickness of aerosols cannot be totally excluded.

We have shown that in the central part of the north permanent cap of Mars, albedo variations in early summer are linked to a major increase in ice grain size, as seasonal frost with grain sizes <100 μm sublimates, so that the larger grains of the permanent ice (~1 mm) dominate the reflectance properties. In a few areas close to the edges of permanent surface ice regions, bright accumulations of small grains survive until late in the summer. In outlying ice-rich regions, the albedo markedly increases whereas the grain size (also ~1 mm) does not change. One month after the summer solstice, old ice is exposed at the surface over most ice-rich areas. This should lead to a net sublimation of ice with the present inclination. The low level of dust contamination of the ice remains to be explained, although there are indications that a clean-up process may be associated with sublimation.

References and Notes

1. H. H. Kieffer, S. C. Chase, T. Z. Martin, R. E. Miner, F. D. Palluconi, *Science* **194**, 1341 (1976).
2. H. H. Kieffer, T. N. Titus, *Icarus* **154**, 162 (2001).
3. D. S. Bass, K. E. Herkenhoff, D. E. Paige, *Icarus* **144**, 382 (2000).
4. P. B. James, B. A. Cantor, *Icarus* **154**, 131 (2001).
5. A. S. Hale, D. S. Bass, L. K. Tamppari, *Lunar Planet. Sci.* **34**, 1422 (2003).
6. M. C. Malin, K. S. Edgett, *J. Geophys. Res.* **106**, 23429 (2001).
7. H. H. Kieffer, *J. Geophys. Res.* **95**, 1481 (1990).
8. J.-P. Bibring *et al.*, *Science* **307**, 1576 (2005); published online 17 February 2005 (10.1126/science.1108806).
9. The visible part of the range would be useful for constraining surface dust content and composition. However, the visible channel (0.4 to 1 μm) still has some calibration problems, and atmospheric aerosols have a major influence at short wavelengths.
10. W. M. Calvin, T. N. Titus, *Lunar. Planet. Sci.* **35**, 1455 (2004).
11. S. Douté, B. Schmitt, *J. Geophys. Res.* **103**, 31367 (1998).
12. F. Poulet, J. N. Cuzzi, D. P. Cruikshank, T. Roush, C. M. Dalle Ore, *Icarus* **160**, 313 (2002).
13. Y. Shkuratov, L. Starukhina, H. Hoffmann, G. Arnold, *Icarus* **137**, 235 (1999).
14. W. M. Grundy, B. Schmitt, *J. Geophys. Res.* **103**, 25809 (1998).
15. M. A. Mischna, M. I. Richardson, R. J. Wilson, D. J. McCLeese, *J. Geophys. Res.* **108**, 5062 (2003).
16. B. Levrard, F. Forget, F. Montmessin, J. Laskar, *Nature* **431**, 1072 (2004).
17. A. W. Nolin, *J. Geophys. Res.* **103**, 25851 (1998).
18. This work was supported by CNES, CNRS, and Université Paris XI.

5 January 2005; accepted 7 February 2005
Published online 17 February 2005;
10.1126/science.1109438
Include this information when citing this paper.

REPORT

Sulfates in the North Polar Region of Mars Detected by OMEGA/Mars Express

Yves Langevin,* François Poulet, Jean-Pierre Bibring, Brigitte Gondet

The Observatoire pour la Minéralogie, l'Eau, les Glaces, et l'Activité (OMEGA) imaging spectrometer observed the northern circumpolar regions of Mars at a resolution of a few kilometers. An extended region at 240°E, 85°N, with an area of 60 kilometers by 200 kilometers, exhibits absorptions at wavelengths of 1.45, 1.75, 1.94, 2.22, 2.26, and 2.48 micrometers. These signatures can be unambiguously attributed to calcium-rich sulfates, most likely gypsum. This region corresponds to the dark longitudinal dunes of Olympia Planitia. These observations reveal that water alteration played a major role in the formation of the constituting minerals of northern circumpolar terrains.

The northern circumpolar regions of Mars constitute a complex geological region. Permanent ice deposits partially cover a bulge attributed to a water ice cap, as well as some low-altitude outlying regions down to latitudes of ~70°N. Intermixed with these bright areas, layered terrains and dark circumpolar sand deposits are observed. This entire region is a young complex system of layered deposits of ice and dust, plains, and dunes (*1*). The role of liquid water in the origin of these complex structures has been debated, either as outflows (*2*) or as large standing bodies of water (*3*, *4*). Mineralogical information is needed to constrain the geological history of these regions. Few unambiguous signatures have been observed in the northern circumpolar regions

Institut d'Astrophysique Spatiale (IAS), Bâtiment 121, 91405 Orsay Campus, France.

*To whom correspondence should be addressed. E-mail: yves.langevin@ias.u-psud.fr

by previous experiments dedicated to mineralogical studies (*5*, *6*).

The OMEGA visible and near-infrared imaging spectrometer has been operating around Mars since January 2004. This instrument maps 352 wavelengths from 0.35 to 5.1 μm (*7*, *8*). A series of 11 observations obtained between 13 and 24 October 2004, corresponding to heliocentric longitude L_s 100° to 105° (northern summer), provides comprehensive coverage of the regions above 73°N. A composite of the 11 observations (Fig. 1) combines information on the reflectance in the continuum at 1.085 μm (gray scale) with the strength of an absorption feature at 1.927 μm. An irregular crown of low-albedo regions corresponding to the dark circumpolar dunes is observed around the regions dominated by water ice and layered deposits. The absorption at 1.927 μm is defined relative to a continuum at 1.857 μm and 2.136 μm. These three wavelengths have been selected so as to lie out of the main atmospheric CO_2 absorption bands. The regions with exposed ice (*9*) are left in white. A region where the absorption at 1.927 μm is larger than 20% (orange-red area in Fig. 1) is identified close to 240°E, 80°N. The extent of this region, which has a mean reflectance of 16% at 1.08 μm, is ~60 km by 140 km. This spectral signature is observed on only a small fraction of the dark circumpolar dunes (Fig. 1). The corresponding spectral unit lies close to the outer boundary of the permanent surface ice.

A representative reflectance spectrum from a 10 km by 10 km spectrally homogeneous region centered at 244.5°E, 80.2°N is shown in Fig. 2. This region lies 4.9 km below the Mars Orbiter Laser Altimeter (MOLA) reference surface; hence, strong atmospheric absorption features are observed, in particular at 2 μm. As a first approximation, atmospheric absorption features can be removed by dividing the reflectance spectrum by a ratio of spectra of homogeneous terrains obtained by OMEGA on Olympus Mons, scaled to the same column density of CO_2. The reflectance spectrum corrected from atmospheric absorption (red spectrum in Fig. 2) exhibits a strong absorption feature at ~1.94 μm and weaker signatures at other wavelengths. The 1.94-μm absorption feature is far stronger (>25%) than the closest atmospheric H_2O feature at 1.875 μm (<2%). Spectra from most other dark circumpolar areas are characterized by a much weaker and broader absorption feature also centered close to 1.94 μm. When mapping the strength of the 1.94-μm absorption feature in Fig. 1, we did not select the OMEGA spectral channel closest to maximum absorption (1.941 μm) but instead chose that at the next lower wavelength (1.927 μm), because atmospheric CO_2 absorption is much smaller at 1.927 μm (~2%) than at 1.941 μm (~10%). The spatial distribution of weaker features (e.g., at 2.48 μm and 1.75 μm) is highly consistent with that of the 1.94-μm absorption feature, which demonstrates that a single constituent is responsible for these spectral signatures over the whole region.

We applied a spectral ratio method so as to consolidate our mineral identification. We divided the blue spectrum from Fig. 2 (before atmospheric correction) by the reflectance spectrum of a region with a similar albedo and altitude that did not exhibit a narrow signature. The spectral ratio (red curve in Fig. 3) does not depend on knowledge of the OMEGA photometric function. The main atmospheric bands have a small impact on this spectral ratio, because the altitudes of the two regions are similar (4.9 km and 4.4 km, respectively, below the MOLA reference surface), except for possible spatial variations in water vapor content (at most a few percent in band strength). The spectral features that are observed in the normalized ratio are similar to that of the reflectance spectrum of Fig. 2, which shows that the observed strong signature at 1.94 μm is not an artifact resulting from the OMEGA photometric function or the atmospheric correction procedure.

In Fig. 3, we also show the ratio of two spectra obtained by OMEGA during ground calibration: that of a gypsum powder with grain sizes < 40 μm and that of an aluminum oxide powder, which is spectrally featureless in this wavelength range. The match in terms of position and relative strength of the minor and major features between the Mars spectral ratio and the calibration spectral ratio constitutes an unambiguous detection of gypsum ($CaSO_4 \cdot 2H_2O$) as a major constituent of the hydrated region observed close to 245°E, 80°N. Less hydrated calcium sulfates, such as bassanite ($2CaSO_4 \cdot H_2O$), would also provide a good match with the observed spectral signature, but the fit is definitely less satisfactory, in particular for the small spectral

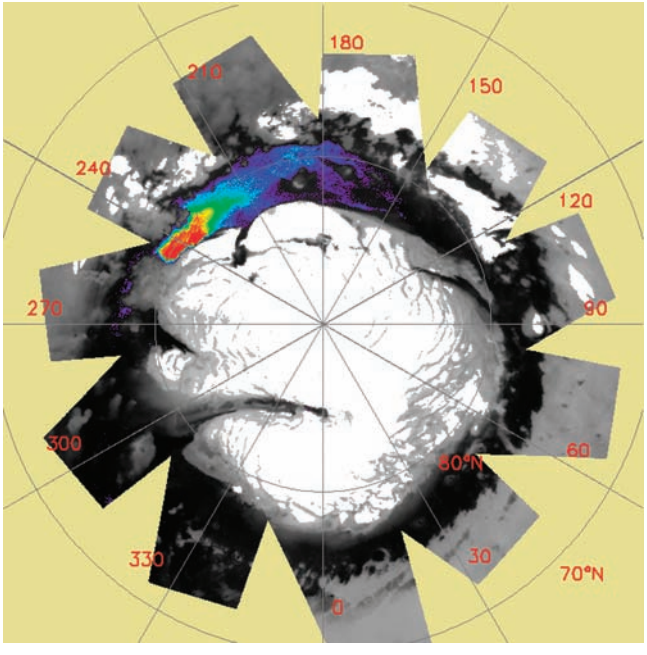

Fig. 1. Composite map of 11 OMEGA observations obtained in October 2004. The gray scale corresponds to the albedo at 1.085 μm (continuum), with a range from black (10%) to light gray (35%). False-color information is superimposed for areas exhibiting an absorption feature at 1.927 μm, with a rainbow color scale from 6% (purple) to >25% (red) in terms of band strength. White areas correspond to the regions where OMEGA observes water ice at the surface, which are defined by a water ice band strength at 1.5 μm exceeding 20% (*9*).

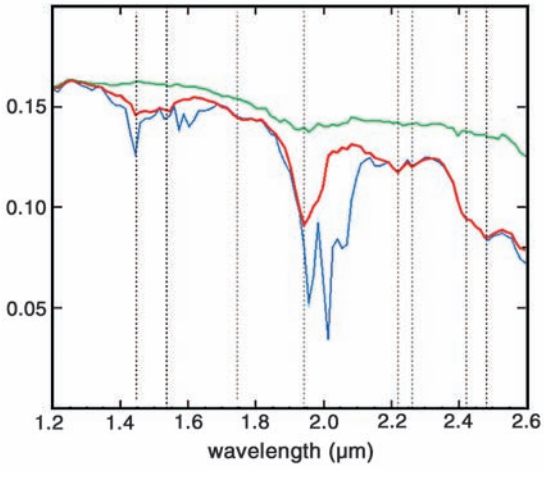

Fig. 2. Reflectance spectra. Blue curve, reflectance spectrum of the region exhibiting the strongest absorption at 1.94 μm (244.5°E, 80.2°N); red curve, blue spectrum corrected for atmospheric absorption; green curve, reference spectrum of a dark region of similar elevation and albedo (54.9°E, 78.2°N) that does not exhibit a strong and narrow signature at 1.94 μm, corrected for atmospheric absorption. Absorption features are observed at 1.445, 1.535, 1.745, 1.94, 2.22, 2.26, 2.42, and 2.48 μm (dotted lines) in the red spectrum.

features observed at 1.445, 1.535, 2.22, 2.26, and 2.42 μm. Fine-grained gypsum is bright (reflectance >40% in the continuum). Therefore, the observed reflectance of 16% at 1.1 μm requires an admixture of opaque and spectrally neutral material such as magnetite.

The gypsum signature is spatially correlated to dark longitudinal dunes (*1*) that belong to Olympia Planitia, the largest sand sea on Mars. Both physical and morphological properties led to the idea that the Olympia dunes were formed at their present location: MOLA topography reveals that most of Olympia Planitia has a convex topography and appears to underlie the present polar cap and associated deposits (*10*). Furthermore, the Olympia dune field has a much lower thermal inertia than other Martian dunes, which supports the idea that it consists of aggregates of μm-sized particles (*11*, *12*). Such small particles could be easily transported via atmospheric suspension, and other sources for dune material have been proposed, such as pyroclastic ash and oceanic or outflow sediment (*10*). However, transportation of dust and sand from distant sources in the present low-pressure atmosphere is unlikely (*12*). Byrne and Murray (*13*) have identified a platy unit distinct from the layered deposits at the base of the present layered deposits. The regions where this unit is exposed at the surface are correlated with the occurrences of dune bed forms, leading these authors to the conclusion that the dune material is derived from in situ erosion of the platy unit.

The calcium sulfate component observed by OMEGA supports the hypothesis that the constitutive material of the dunes was formed in a different environment than the other polar terrains, most likely before the emplacement of the present-day polar cap (*13*, *14*). The formation of calcium sulfates requires an interaction between water and pyroxenes or feldspars in a sulfur-rich environment. Volcanic processes provide the most likely supply of sulfur (H_2S, SO_2, or sulfur-rich pyroclastic ashes). Several processes can be considered for the formation of sulfates, involving surface weathering, groundwater circulation in buried sediments, acid snow or rain falling on basalt, or evaporation of standing bodies of water.

An increase in planetary obliquity may have increased the quantity of water vapor in the atmosphere and the abundance of water ice clouds in the polar region (*15*), so that circumpolar terrains may have undergone strong atmospheric weathering. However, the alteration signature observed in bright terrains is quite different from that of the sulfate-rich region, with no absorption at either 1.75 μm or 1.94 μm. Furthermore, the supply of sulfur is not straightforward in this hypothesis. The formation of sulfate minerals on Mars could also occur through oxidative weathering of iron sulfides (*16*, *17*). The prerequisite for such a weathering scenario is a wide distribution of sulfides. If this weathering process has occurred on Mars in the past, large quantities of sulfates should have been formed. This would require the weathered material to be exposed on only a small fraction of the planet, where OMEGA can detect it (*8*).

Groundwater related to hydrothermal sources or local volcanism is not a likely formation process for the observed sulfate-rich unit, as no clear geological evidence has been found for volcanic activity in circumpolar regions. Apart from local geothermal hot spots, other scenarios such as basal melting at high pressure under thick deposits of dust and ice have been proposed as possible explanations for groundwater-related processes [e.g., (*18*)].

The interaction of basalts with acidic snow has been proposed as a candidate for the formation of sulfates in Noachian terrains (*8*, *19*). Such a process requires extended episodes of volcanic activity. The small extent of the sulfate-rich unit is difficult to reconcile with a volcanic episode during which the whole region would have been exposed to acidic snows, unless this unit represents a small fraction of a much larger area that was recently uncovered by erosion.

The observed sulfate-rich unit could also result from outflows from an ice cap during a warm climatic excursion. The sulfates would then result from the evaporation of water saturated with salts after prolonged interactions with sulfur-rich material and crustal rocks. Such hypersaline conditions would extend the stability zone of the liquid phase near the surface to colder temperatures. If this interpretation is correct, our results provide strong evidence for climatic episodes compatible with the presence of surface water, as advocated by Pathare and Paige (*20*) during periods of high obliquity (>45°).

The mineralogical signature of gypsum observed by OMEGA in a specific region close to the permanent north polar cap provides strong evidence for alteration processes involving water on the surface of Mars. Possible hypotheses for the formation of this unit involve the interaction of acidic snow with calcium-rich minerals during an extensive episode of volcanic activity, major outflows followed by evaporation of salt-rich water (possibly predating the formation of the present-day ice cap), or a combination of these two processes.

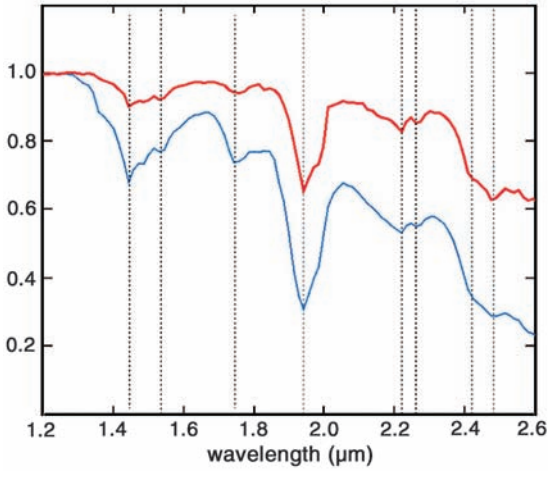

Fig. 3. Normalized spectral ratios. Red curve, ratio of the blue spectrum in Fig. 2 divided by the raw reflectance spectrum of the reference region (corresponding to the green spectrum in Fig. 2 without the atmospheric correction), normalized to 1 at 1.25 μm; blue curve, normalized ratio of the spectra of gypsum and aluminum oxide obtained by OMEGA during ground calibration. Features are observed in both spectral ratios at 1.445, 1.535, 1.745, 1.94, 2.22, 2.26, 2.42, and 2.48 μm (dotted lines).

References and Notes

1. K. Tanaka, D. Scott, *USGS Misc. Invest. Ser. Map I-1802-C* (1987).
2. V. R. Baker, M. Carr, V. Gulick, C. Williams, M. Marley, in *Mars*, H. Kieffer *et al.*, Eds. (Univ. of Arizona Press, Tucson, AZ, 1992), pp. 493–522.
3. T. Parker, R. Saunders, D. Schneeberger, *Icarus* **82**, 111 (1989).
4. S. Clifford, T. Parker, *Lunar Planet. Sci. Conf.* **30**, abstract 1619 (1999).
5. M. B. Wyatt, K. L. Tanaka, *3rd International Conference on Mars Polar Science and Exploration* (Lake Louise, Alberta, Canada, 13 to 17 October 2003), abstract 8118.
6. S. Ivanov *et al.*, *6th International Conference on Mars* (Pasadena, CA, 20 to 25 July 2003), abstract 3182.
7. J.-P. Bibring *et al.*, *ESA Spec. Pub. 1240*, 37 (2004).
8. J.-P. Bibring *et al.*, *Science* **307**, 1576 (2005).
9. Y. Langevin *et al.*, *Science* **307**, 1581 (2005); published online 17 February 2005 (10.1126/science.1109438).
10. K. E. Fishbaugh, J. W. Head, *J. Geophys. Res.* **105**, 22455 (2000).
11. D. A. Paige, J. E. Bachman, K. D. Keegan, *J. Geophys. Res.* **99**, 25959 (1994).
12. K. E. Herkenhoff, A. R. Vasavada, *J. Geophys. Res.* **104**, 16487 (1999).
13. S. Byrne, B. C. Murray, *J. Geophys. Res.* **107**, 10.1029/2001JE001615 (2002).
14. K. E. Fishbaugh, J. W. Head III, *Lunar Planet. Sci. Conf.* **25**, abstract 1156 (2004).
15. M. A. Mischna, M. I. Richardson, R. J. Wilson, D. J. McGleese, *J. Geophys. Res.* **108**, 10.1029/2003JE002051 (2003).
16. R. G. Burns, D. S. Fisher, *J. Geophys. Res.* **95**, 14415 (1990).
17. J. L. Bishop, P. Schiffman, M. D. Lane, M. D. Dyar, *Int. J. Astrobiol.*, in press.
18. S. Clifford *et al.*, *Icarus* **144**, 210 (2000).
19. A. Gendrin *et al.*, *Science* **307**, 1587 (2005).
20. A. V. Pathare, D. A. Paige, *1st International Conference on Mars Polar Science and Exploration* (Camp Allen, TX, 18 to 22 October 1998), abstract 953.
21. Supported by Centre National d'Etudes Spatiales, CNRS, and Université Paris Sud.

23 December 2004; accepted 4 February 2005
Published online 17 February 2005;
10.1126/science.1109091
Include this information when citing this paper.